

---

# Climate Data Record (CDR) Program

## Climate Algorithm Theoretical Basis Document (C-ATBD) for GPSRO Calibrated TLS Temperatures



CDR Program Document Number: CDRP-ATBD-0098  
Originator Document Number: N/A  
Revision 2 / July 26, 2013

**REVISION HISTORY**

| <b>Rev.</b> | <b>Author</b>   | <b>DSR No.</b> | <b>Description</b>                            | <b>Date</b> |
|-------------|-----------------|----------------|---|-------------|
| 1           | Shu-peng Ben Ho | DSR-103        | Initial Submission to CDR Program             | 07/26/2011  |
| 2           | Shu-peng Ben Ho | DSR-445        | Algorithm updated with changes to input data. | 07/26/2013  |
|             |                 |                |   |             |
|             |                 |                |   |             |
|             |                 |                |   |             |
|             |                 |                |   |             |
|             |                 |                |   |             |
|             |                 |                |   |             |
|             |                 |                |   |             |
|             |                 |                |   |             |

## TABLE of CONTENTS

|   |           |
|---|-----------|
| <b>1. INTRODUCTION.....</b>                         | <b>6</b>  |
| 1.1 Purpose.....                                    | 6         |
| 1.2 Definitions.....                                | 6         |
| 1.3 Document Maintenance.....                       | 7         |
| <b>2. OBSERVING SYSTEMS OVERVIEW.....</b>           | <b>8</b>  |
| 2.1 Products Generated .....                        | 8         |
| 2.2 Instrument Characteristics .....                | 8         |
| <b>3. ALGORITHM DESCRIPTION.....</b>                | <b>9</b>  |
| 3.1 Algorithm Overview .....                        | 9         |
| 3.2 Processing Outline.....                         | 9         |
| 3.3 Algorithm Input.....                            | 12        |
| 3.3.1 Primary Sensor Data .....                     | 12        |
| 3.3.2 Ancillary Data.....                           | 12        |
| 3.3.3 Derived Data .....                            | 13        |
| 3.3.4 Forward Models.....                           | 14        |
| 3.4 Theoretical Description .....                   | 15        |
| 3.4.1 Physical and Mathematical Description.....    | 16        |
| 3.4.2 Data Merging Strategy.....                    | 17        |
| 3.4.3 Numerical Strategy .....                      | 17        |
| 3.4.4 Calculations.....                             | 17        |
| 3.4.5 Look-Up Table Description.....                | 17        |
| 3.4.6 Parameterization .....                        | 17        |
| 3.4.7 Algorithm Output.....                         | 18        |
| <b>4. TEST DATASETS AND OUTPUTS.....</b>            | <b>19</b> |
| 4.1 Test Input Datasets .....                       | 19        |
| 4.2 Test Output Analysis .....                      | 21        |
| 4.2.1 Reproducibility.....                          | 21        |
| 4.2.2 Precision and Accuracy .....                  | 21        |
| 4.2.3 Error Budget.....                             | 24        |
| <b>5. PRACTICAL CONSIDERATIONS.....</b>             | <b>25</b> |
| 5.1 Numerical Computation Considerations.....       | 25        |
| 5.2 Programming and Procedural Considerations ..... | 25        |
| 5.3 Quality Assessment and Diagnostics .....        | 25        |
| 5.4 Exception Handling .....                        | 27        |
| 5.5 Algorithm Validation .....                      | 28        |
| 5.6 Processing Environment and Resources .....      | 29        |
| <b>6. ASSUMPTIONS AND LIMITATIONS .....</b>         | <b>30</b> |

**6.1 Algorithm Performance..... 30**

**6.2 Sensor Performance..... 30**

**7. FUTURE ENHANCEMENTS..... 31**

**7.1 Enhancement 1 ..... 31**

**7.2 Enhancement 2 ..... 31**

**8. REFERENCES..... 32**

**APPENDIX A. ACRONYMS AND ABBREVIATIONS..... 34**

## LIST of FIGURES

- Figure 1: Flow chart of processing steps to using GPS RO simulated AMSU TLS (channel 9) to calibrate AMSU data from multiple AMSU missions and construct the TLS climate data records. .... 11
- Figure 2: AMSU Channel 9 Atmospheric weighting functions for a typical atmospheric profile in the Tropics and the Arctic, respectively. The weighting function is defined as  $d(\text{transmittance})/d\ln(p)$ . ..... 13
- Figure 3: Flow chart of the procedures to use RO data to AMSU forward model to compute the simulated AMSU channel 9 Tbs. .... 15
- Figure 4: The raw AMSU channel 9 Tbs from NOAA 16 reported for November 2002 for (a) the only day of AMSU Tbs with two obviously bad tracks, (b) the monthly mean AMSU channel 9 including all NOAA 16 AMSU Tbs in the same month, and (c) the same as (b), except that it only includes pixels with high quality flags. .... 20
- Figure 5: Comparison of (a) synthetic CHAMP Tbs and AMSU N18 Ch9 Tbs, (b) COSMIC calibrated N18 AMSU Tbs and CHAMP calibrated N18 AMSU Tbs, (c) synthetic CHAMP Tbs and AMSU N16 Ch9 Tbs, and (d) COSMIC calibrated N16 AMSU Tbs and CHAMP calibrated N16 AMSU Tbs. .... 24
- Figure 6: The global monthly map in a 2.5 degree x 2.5 degree grid on January 2004 for (a) RO-simulated AMSU TLS, (b) RSS, (c) UAH, and (d) SNO. .... 26
- Figure 7: The time series of the TLS difference for RSS-RO\_AMSU, UAH-RO\_AMSU, and SNO-RO\_AMSU for (a) the entire globe (82.5°N-82.5°S, the left upper panel), (b) the 82.5°N-60°N zone (the upper right panel), (c) the 60°N-20°N zone (the middle left panel), (d) the 20°N-20°S zone (the middle right panel), (e) the 20°S-60°S zone (the bottom left panel), and (f) the 60°S-82.5°S zone (the bottom right panel).. 27
- Figure 8: Comparison of COSMIC-calibrated N15 Tbs and N16-calibrated N15 Tbs. The best fit is in dash line. Diagonal one-to-one fit is in gray solid line. .... 28

# 1. Introduction

## 1.1 Purpose

The purpose of this document is to describe the algorithm submitted to the National Climatic Data Center (NCDC) by Dr. Shu-peng Ben Ho/COSMIC UCAR. This algorithm produces Advanced Microwave Sounder Unit (AMSU) temperatures in the lower stratosphere (TLS, e.g., AMSU channel 9) from National Oceanic and Atmospheric Administration (NOAA), National Aeronautics and Space Administration (NASA), and Europe METeorological Operational satellite-A (Metop/A) satellites which have been calibrated using coincident Global Positioning System (GPS) Radio Occultation (RO) temperature profile measurements from Constellation Observing System for Meteorology, Ionosphere, and Climate (COSMIC) and Challenging Mini-satellite Payload (CHAMP), and Gravity Recovery And Climate Experiment (GRACE). The actual algorithm is defined by the computer program (CDR\_ch9\_V1.1 package) that accompanies this document, and thus the intent here is to provide a guide to understanding that algorithm, from both a scientific perspective and in order to assist a software engineer or end-user performing an evaluation of the code.

For examples of existing C-ATBDs, please see the “Algorithm Description” links at <http://www.ncdc.noaa.gov/cdr/operationalcdrs.html>, and in particular that for the AMSU-A Ch9 Brightness Temperature CDR, at <http://www1.ncdc.noaa.gov/pub/data/sds/cdr/docs/ro-amsu-ch9-catbd.pdf>.

## 1.2 Definitions

Following is a summary of the symbols used to define the algorithm.

Atmospheric parameters:

$$T = \text{Temperature} \quad (1)$$

$$P = \text{Pressure} \quad (2)$$

$$P_w = \text{Vapor Pressure} \quad (3)$$

$$N = \text{Refractivity} \quad (4)$$

$$T_b = \text{Brightness Temperature} \quad (5)$$

## **1.3 Document Maintenance**

This document describes the submission, version 1.1, of the processing algorithm and resulting data. The version number will be incremented for any subsequent enhancements or revisions.

## **2. Observing Systems Overview**

### **2.1 Products Generated**

The objective of this algorithm is to use GPS RO data to serve as climate benchmark to calibrate AMSU measurements in order to constrain the uncertainties of AMSU-inferred TLS trends. Monthly averages over a 9-year period from May 2001 through December 2012 from the combined contributions of AMSU measurements from NOAA, NASA, and MetOp-A polar orbiters are calculated on a 2.5 degree x 2.5 degree grid. The final product consists of monthly mean averages of calibrated AMSU channel 9 measurements, a mean monthly climatology calculated using 12 full years of data, and monthly anomaly values.

### **2.2 Instrument Characteristics**

GPS RO data are highly recommended by the National Science Council (NRC, 2007), the World Meteorological Organization (WMO, 2007), and Global Climate Observing System (GCOS, 2004) as an important component of the global observing system. GPS RO is the only self-calibrated observing technique from space where its fundamental measurement is traceable to the international system of units (SI traceability; Ohring et al., 2007). GPS receivers on low-Earth orbiting (LEO) satellites receive measurable radio frequency signals transmitted from GPS satellites, which, with monitoring and corrections from a series of atomic clocks, allows the GPS time system to be traced to the SI second with a high degree of accuracy. Available GPS RO data from multiple RO missions provide a unique opportunity for monitoring and detecting the vertical structure of atmospheric thermal soundings with high vertical resolution and high accuracy, under all weather conditions.

On board the NOAA series of polar-orbiting satellites, the Microwave Sounding Unit (MSU) and the Advanced Microwave Sounding Unit (AMSU) have also provided near all-weather temperature measurements at different atmospheric vertical layers since 1979 and 1998, respectively. Over the past decade, the roughly 30 years of MSU/AMSU measurements have been extensively used for climate temperature trend detection (Christy et al. 2000, 2003; Mears et al. 2003; Vinnikov and Grody, 2003; Vinnikov et al. 2006; Grody et al. 2004; Zou et al. 2006). Because the MSU/AMSU operational calibration coefficients were obtained from pre-launch datasets (Mo et al. 2001), the orbital changes on MSU/AMSU measurements after launch may not be completely accommodated by these calibration coefficients. Different MSU/AMSU missions may contain different measurement biases, which vary with time and location due to on-orbit heating or cooling of the satellite components. This causes difficulties for climate trend detection (e.g., Christy et al. 2000; Mears et al. 2003; Grody et al. 2004; Zou et al. 2006).

## 3. Algorithm Description

### 3.1 Algorithm Overview

The processing of calibrated AMSU data is achieved by the sequential application of programs, which are divided into four logical steps. First, pixel data for the AMSU brightness temperatures for channel 9 are extracted from the level 1B data sets and stored in daily files for each polar orbiter. In the second step, calibration coefficients are calculated from coincident measurements of AMSU channel 9 brightness temperatures and corresponding values derived from an AMSU forward model applied to temperature profile measurements from GPS RO. For the third step, the monthly calibration coefficients are applied to adjust the AMSU measurements for each polar orbiter to the GPS RO reference. Note that to have enough RO profiles, which contain reasonable temporal and spatial coverage, we use three consecutive months of CHAMP data to represent the TLS variation for the middle month. Three monthly running CHAMP-AMSU pairs are used before June 2006, whereas the available CHAMP, COSMIC, and GRACE RO data in the same month are used to match up with the AMSU data after June 2006. The calibrated AMSU measurements are then combined into a single dataset of gridded monthly values. From these the climatology is calculated using 9 years of data. Anomaly values are then obtained by subtracting this climatology from the monthly values. The final step is to convert and combine the data into netCDF files containing the final product.

### 3.2 Processing Outline

The four processing steps are indicated in Figure 1. Input data, indicated by the blue boxes, are acted upon by discrete programs to generate intermediate output files as indicated. In greater detail, these steps which lead to the final output product indicated by the green box are:

**STEP(1) Pre-Processing:** The level 1B data from the polar orbiters are extracted using two IDL (Interface description language) programs. Data from NOAA and METOP orbiters are obtained from the program '*extract noaa amsu.pro*'. The user must edit this program to specify the name of the polar orbiter, the time interval of data to process, and the input/output paths for the datasets. The program is then compiled and run separately in IDL for each orbiter. The data from the AQUA orbiter has a different format and requires a separate IDL program, '*extract aqua amsu.pro*'. After running these, the extracted values for each orbiter are stored into daily ASCII files for later use.

**STEP(2) Calculation of Calibration Coefficients:** For each GPS RO mission, channel 9 brightness temperatures ( $T_b$ ) are calculated from vertical profiles of temperature using an AMSU forward model (see Figure 2).

The set of AMSU measurements from each NOAA polar orbiter that are coincident with these derived values are obtained from the IDL program '*match gps noaa.pro*'. The user must edit this program to specify the names of the GPS RO mission and NOAA orbiter, the time interval of data to process, and the tolerances used to determine coincidence. The program is then compiled and run separately in IDL for each combination of NOAA orbiter and GPS RO mission to obtain daily matched measurements. A separate program, '*match gps aqua.pro*', is used to obtain the matched measurements for the AQUA orbiter. The criteria used to obtain coincident values are 30 minutes in time, 50 km spatial distance, and a scan angle tolerance of 15 degrees. The resulting matched data are stored in daily ASCII files for later use.

Once these datasets are generated for each GPS RO mission and polar orbiter have been generated, then the coincident measurements from all available GPS RO missions are used to calculate the monthly calibration coefficients for each individual polar orbiter. For the NOAA and METOP orbiter, the matched measurements for the specified set of RO missions are used to calculate linear fit coefficients for each month using the IDL program '*offset slope multigps noaa month.pro*'. The user must edit this program to specify the polar orbiter, the set of RO missions to use, the time interval of data to process, and the matching tolerances that may optionally be more restrictive than those used in the matching program. The program is then compiled and run separately in IDL for each orbiter to store the monthly fit coefficients. A separate program '*offset slope multigps aqua month.pro*' is used to obtain the linear fit values for the AQUA orbiter. The resulting monthly fit coefficients for each orbiter are stored in ASCII files for later use.

**STEP(3) Apply Calibration:** Prior to application of the linear calibration, monthly means of AMSU channel 9 brightness temperatures for each NOAA orbiter on a 2.5 degree x 2.5 degree grid are calculated by the IDL program '*bin noaa monthlymean.pro*'. The user must edit the program to specify the orbiter name, the AMSU channel number, and the time interval of data to process. The program is then compiled and run in IDL to generate the monthly mean data files for each orbiter. A separate program '*bin aqua monthlymean.pro*' is used to calculate monthly gridded means for the AQUA orbiter. The resulting monthly mean grids are stored in ASCII files for later use.

The calibration coefficients for each polar orbiter are then applied to the monthly mean gridded values to obtain the monthly adjusted AMSU channel 9 brightness temperatures. The program, '*convert amsu bygps.pro*', which is compiled and run separately for each orbiter, reads in the linear fit coefficients and uses them to adjust the corresponding monthly gridded values. The adjusted monthly mean grids are then stored in ASCII files for later use.

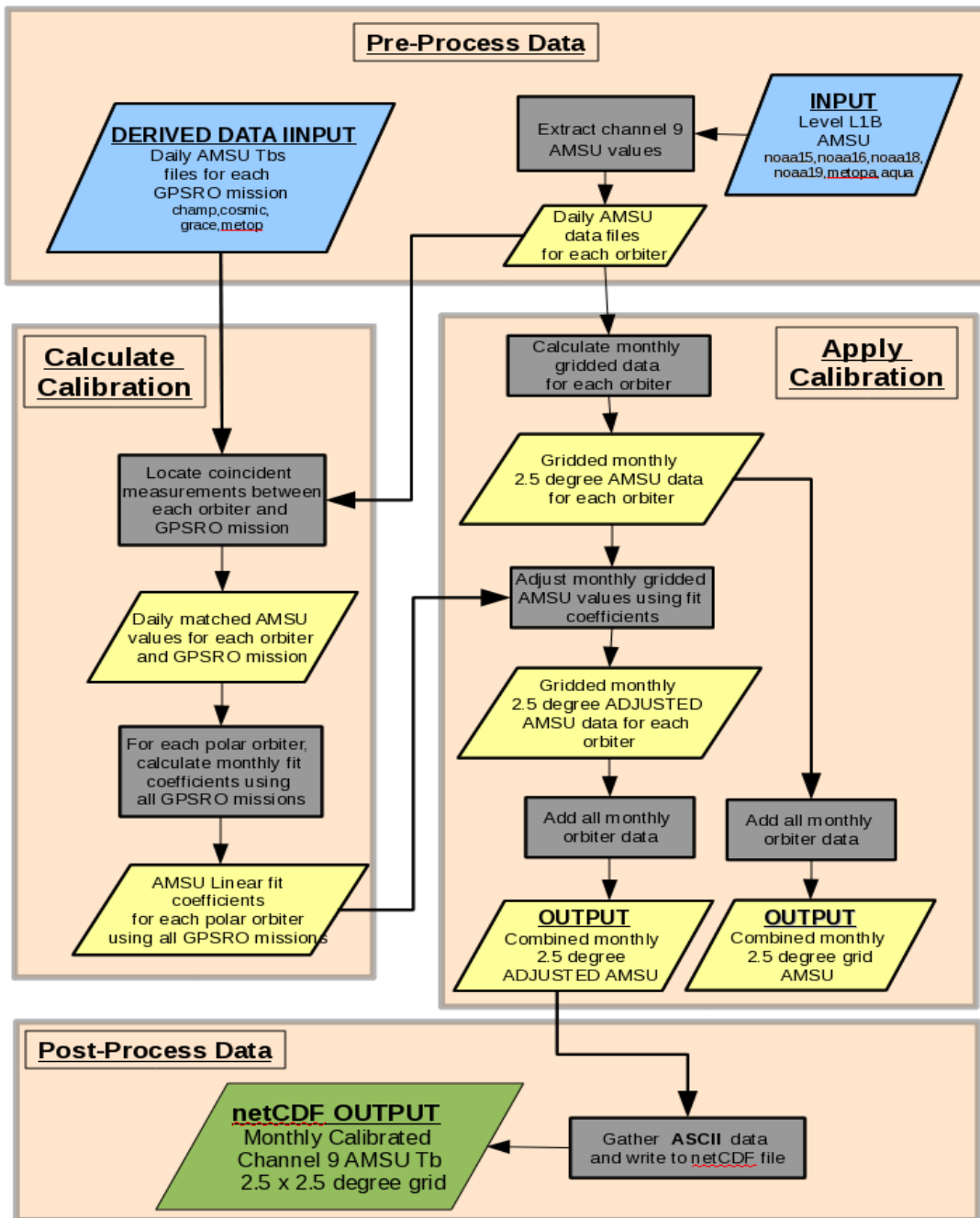


Figure 1: Flow chart of processing steps to using GPS RO simulated AMSU TLS (channel 9) to calibrate AMSU data from multiple AMSU missions and construct the TLS climate data records.

Once all of the monthly gridded values have been calibrated, the IDL program '*combine\_amsu.pro*' reads in the monthly gridded values for the specified set of polar orbiters and averages the values to generate combined monthly gridded values for AMSU channel 9. The resulting monthly mean grids are stored in ASCII files for later use.

Climatology and anomaly values are calculated by the IDL program '*generate\_climatology\_anomaly.pro*'.

**STEP(4) Post-Processing:** The resulting combined monthly gridded data are written to the final V4 netCDF datasets by the FORTRAN programs: '*gen\_netCDF\_monthly.exe*', '*gen\_netCDF\_climatology.exe*', and '*gen\_netCDF\_anomaly.exe*'.

## 3.3 Algorithm Input

### 3.3.1 Primary Sensor Data

Level 1B AMSU data from NOAA 15, 16, 18, and 19, and from METOP/A, and version 5.0 data from AQUA are used. For each orbiter, AMSU channel 9 brightness temperature, latitude, longitude, time, and scan angle values are input into the algorithm. For each month, the level 1B AQUA data requires 4.0Gb of space while the other polar orbiters requires about 1.0 Gb each. AMSU level 1B data for NOAA and METOP orbiters are available from the NOAA website <http://www.class.noaa.gov/nsaa/products/welcome>. The data from AQUA is available from the NASA website [http://disc.sci.gsfc.nasa.gov/AIRS/data-holdings/by-data-product/amsuL1B\\_Rad.shtml](http://disc.sci.gsfc.nasa.gov/AIRS/data-holdings/by-data-product/amsuL1B_Rad.shtml).

From CDACC VERSION 2010.2640 data, dry temperature and water vapor profiles are obtained from ATM and WET data respectively. The profiles from the GPS RO missions COSMIC and CHAMP are first interpolated to 100 pressure levels and then passed to an AMSU forward model to calculate the corresponding channel 9 brightness temperatures. Those derived brightness temperatures, along with latitude, longitude, and time values, are then input into the algorithm. The size of the derived datasets varies with the number of radio occultation events, typically they require about 10 mb per month. All GPSRO profiles were downloaded from the UCAR COSMIC Data Analysis and Archive Center (CDAAC) (<http://cosmic.cosmic.ucar.edu/cdaac/index.html>).

### 3.3.2 Ancillary Data

N/A

### 3.3.3 Derived Data

The shape and the magnitude of AMSU temperature weighting function (WF) is a function of the temperature profile (Fig. 2), so using an AMSU forward model enables one to reduce WF representation errors in the simulated Tbs as compared to those computed from a globally-fixed WF. The forward model MWFCIMSS from the Cooperative Institute for Meteorological Satellite Studies (CIMSS) was operationally employed in the International ATOVS Processing Package developed at Space Science Engineer Center (SSEC), University of Wisconsin. The validation of microwave transmittance of this model is described in Woolf et al. 1999.

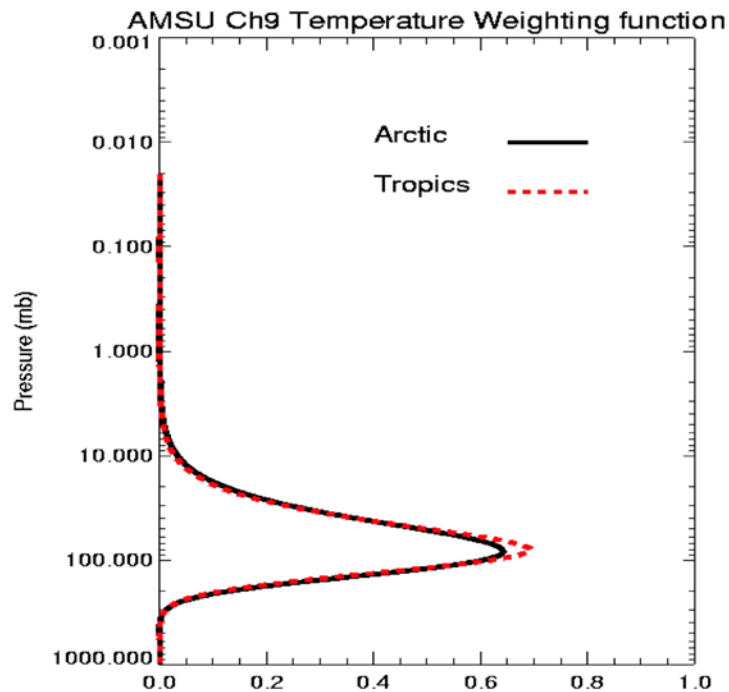


**Figure 2: AMSU Channel 9 Atmospheric weighting functions for a typical atmospheric profile in the Tropics and the Arctic, respectively. The weighting function is defined as  $d(\text{transmittance})/d\ln(p)$ .**

Because the shape and magnitude of AMSU temperature WF is also a function of viewing geometry, the satellite viewing angle is set to nadir for our calculations.

To perform the conversion of high resolution GPS RO temperature profiles into synthetic microwave Tbs, an AMSU fast forward model with 100 fixed pressure levels from CIMSS (microwave forward model-MWFCIMSS) (Hal Woolf, CIMSS, personal communication, 2005) was used. GPS RO soundings are interpolated to MWFCIMSS levels with reduced vertical resolution.

Instead of using a fixed AMSU9 weighting function, we apply each GPS RO profile to MWFCIMSS to simulate AMSU9 BTs (TLS). This approach ensures that the potential effects of changing TLS weighting functions at various atmospheric temperature structures to calculated Tbs are minimal.

The AMSU forward model is applied in two steps. First the temperature and water vapor profiles are extracted from the CDACC level2 data and interpolated to the 100 pressure levels of the forward model and stored into daily data files for each GPS RO mission. Then the forward model is applied to the profiles in each daily file to produce the derived input for the processing algorithm.

In greater detail the steps are:

**STEP(1) Pre-Processing:** The temperature and water vapor data from GPSRO missions are pre-processed using the IDL program '*extract\_gpsro\_profiles.pro*'. The user must edit this program to specify the name of the GPSRO mission, the time interval of data to process, and the input/output paths for the datasets. The program is then compiled and run separately in IDL for each mission. The extracted profiles for each mission are interpolated to the 100 pressure levels of the AMSU forward model. After missing values are replaced using seasonal standard atmosphere profiles, the results are stored into daily ASCII files for later use.

**STEP(2) Apply AMSU Forward Model:** Temperature and water vapor profiles from GPSRO missions are then passed to the AMSU forward model to calculate brightness temperatures for AMSU channels. The FORTRAN program reads in the profile data for the specified GPSRO mission, for the given time interval. The resulting brightness temperature for each day are written to ASCII files for later use as input to the processing algorithm.

### 3.3.4 Forward Models

In this study, CHAMP RO (from 2001 June to 2008 June), COSMIC (from June 2006 to December 2012) and GRACE data (from March 2007 to December 2012) dry temperature profiles are used to compute the synthetic AMSU Ch9 Tbs. All COSMIC RO dry temperature profiles were downloaded from the UCAR COSMIC Data Analysis and Archive Center (CDAAC). An AMSU fast forward model from the Cooperative Institute for Meteorological Satellite Studies–CIMSS, MWF<sub>CIMSS</sub> (Hal Woolf, CIMSS, personal communication, 2005) is

used to project each COSMIC dry temperature profile into synthetic microwave Tbs. The validation of microwave transmittance of this model is described in Woolf et al. (1999).

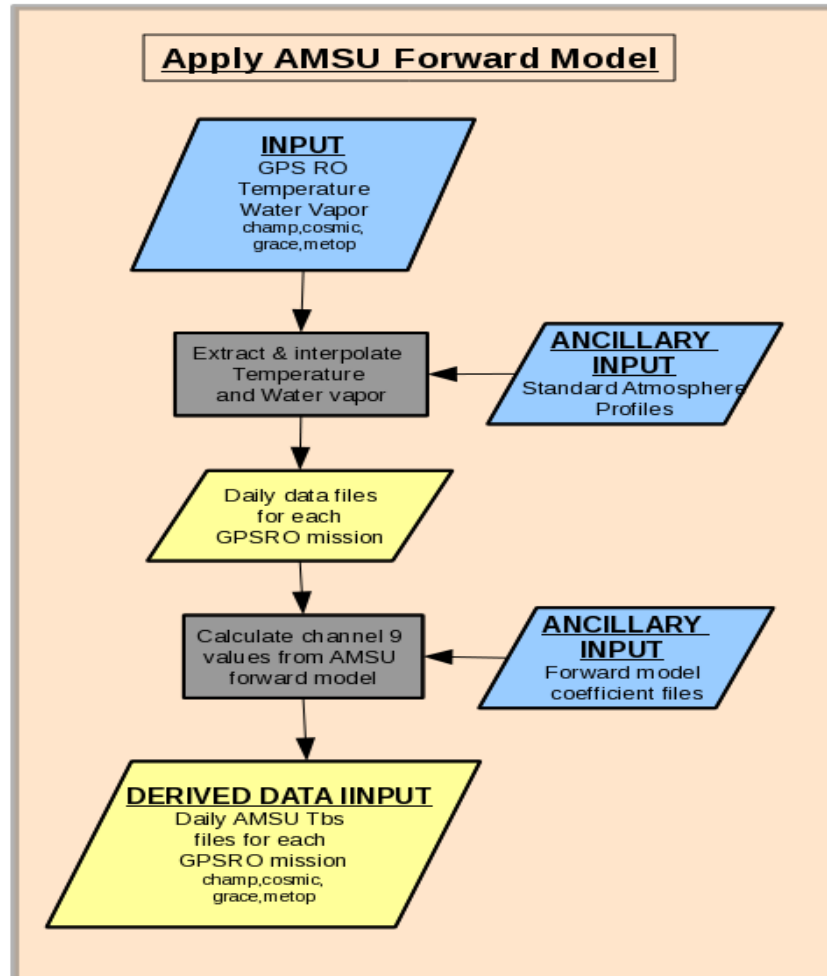


Figure 3: Flow chart of the procedures to use RO data to AMSU forward model to compute the simulated AMSU channel 9 Tbs.

### 3.4 Theoretical Description

The objective of this algorithm is to use GPS RO data to serve as climate benchmark to vicariously calibrate AMSU measurements to constrain the uncertainties of satellite-inferred stratospheric and tropospheric temperature trends.

Because the fundamental observable for the GPS RO technique is of high precision and stability that can be traced to the SI unit of second, RO data do not contain mission-dependent biases. This is demonstrated by the collocated soundings of the CHAMP (launched in 2001) and the COSMIC (launched in 2006) agreeing to within 0.1 K after retrieval (Anthes et al., 2008; Foelsche et al., 2009; Ho et al., 2009a). This makes them potentially useful as a climate benchmark (Ho et al., 2007, 2009c) in addition to being well suited for detecting climate trends (Ho et al., 2009b).

### 3.4.1 Physical and Mathematical Description

Raw RO observations and precise positions and velocities of GPS and LEO satellites, can be used to derive atmospheric refractivity profiles, which are a function of atmospheric temperature and moisture profile (Hajj et al., 2004; Kuo et al., 2004; Ho et al., 2009a). In a neutral atmosphere, the refractivity ( $N$ ) is related to the pressure ( $P$ ), the temperature ( $T$ ) and the partial pressure of water vapor ( $P_w$ ) by the following equation (Bean and Dutton, 1966):

$$N = 77.6 \frac{P}{T} + 3.73 \times 10^5 \frac{P_w}{T^2} \quad (1)$$

The so-called “dry temperature” is obtained by neglecting the water vapor term in equation (1). Above the upper troposphere where moisture is negligible, the dry temperature and the actual temperatures are nearly equal (Ware et al., 1996).

To avoid the spatial and temporal representation errors, we collocate AMSU pixels with each RO profile within 30 minutes and 50 km. AMSU pixels with a satellite viewing angle ranging from -15 degrees to 15 degrees are all included in this study to increase the number of AMSU pixels in our comparison. This approach is unlikely to cause a bias in the analysis, as it is just a random effect at each AMSU-RO pair. To avoid anomalous values due to missing data, differences in brightness temperatures which are larger than 10 degrees are omitted. Collectively these parameters balance the tradeoff between the quality and the number of the matched measurements.

The quality of RO temperatures over the vertical range of AMSU channel 9 sensitivity leads to comparable derived brightness temperatures  $T_{bGPSRO}$ . The highly linear relationship between these and the measured AMSU brightness temperatures  $T_{bAMSU}$ , permits calibration via a simple linear fit:

$$Tb_{\text{AMSU-calibrated}} = \text{SLOPE} \times Tb_{\text{AMSU}} + \text{OFFSET} \quad (2)$$

Where the SLOPE and OFFSET values for each month are calculated by minimizing the RSS between coincident  $Tb_{\text{GPSRO}}$  and  $Tb_{\text{AMSU-calibrated}}$  values.

### **3.4.2 Data Merging Strategy**

Monthly gridded values for each polar orbiter are calculated by binning and averaging pixel level data. The combined monthly average for all polar orbiters is calculated by a simple average of the gridded values from each orbiter.

### **3.4.3 Numerical Strategy**

N/A

### **3.4.4 Calculations**

The calculations primarily consist of binning, averaging, and linear fitting of data points.

### **3.4.5 Look-Up Table Description**

N/A

### **3.4.6 Parameterization**

N/A

### **3.4.7 Algorithm Output**

The algorithm results consist of a set of netCDF files, one for each month over the time interval from May 2001 through December 2012. Each file contains the combined calibrated AMSU channel 9 mean brightness temperatures (K) from available polar orbiters on a 2.5x2.5 degree grid. Also contained in the file are the number of AMSU observations for each gridpoint, the latitudes and longitudes of gridpoints, and the month, year. Each of the files use less than 100Kb.

## **4. Test Datasets and Outputs**

### **4.1 Test Input Datasets**

#### **a. Quality Control of the AMSU Raw Data**

Before using RO-simulated AMSU channel 9 Tbs to calibrate AMSU Tbs from different satellite missions, we need to ensure only high-quality raw AMSU Tbs are used in the calibration processes. By using quality raw data provided by data processing centers, we are able to identify bad satellite tracks on a specific day for each of the individual satellite missions. This quality control procedure is essential to ensure the quality of the binned monthly mean dataset. For example, if one includes all AMSU channel 9 data without checking the quality flags for each of the individual satellite pixels, some obvious bad data from certain tracks (for example, Fig. 4a) will be included in the binning procedures and the binned monthly mean TLS will be highly contaminated (Fig. 4b). The monthly mean TLS, including only AMSU data with good quality flags, is shown in Fig. 4c.

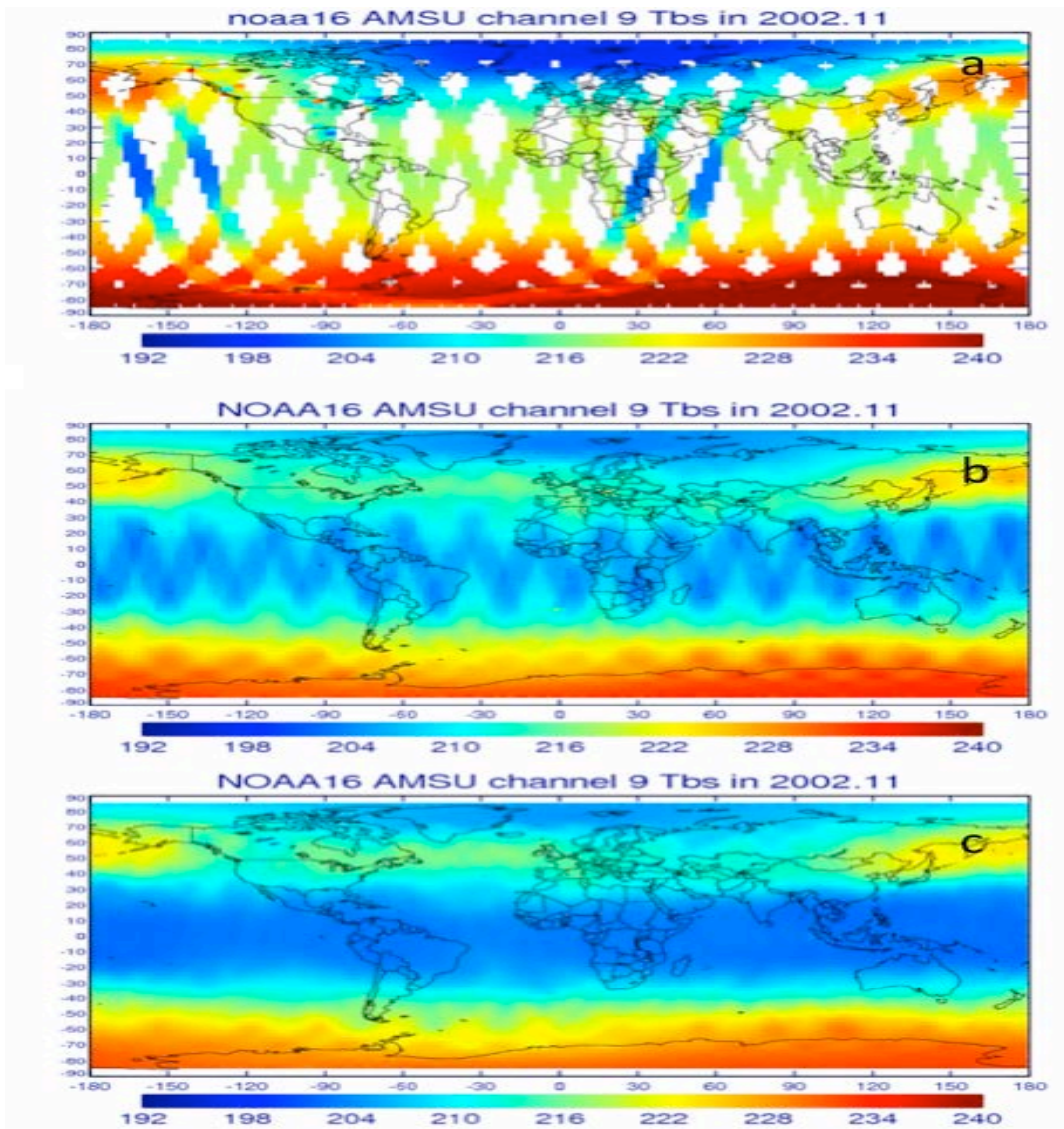


Figure 4: The raw AMSU channel 9 Tbs from NOAA 16 reported for November 2002 for (a) the only day of AMSU Tbs with two obviously bad tracks, (b) the monthly mean AMSU channel 9 including all NOAA 16 AMSU Tbs in the same month, and (c) the same as (b), except that it only includes pixels with high quality flags.

## b. Two Months of Test Data

Two months of test data from November and December of 2006 are provided with the IDL and FORTRAN source programs. The directory `$SRC/Test-Data/Input/AMSU/` contains sub-directories containing L1B polar orbiter data for NOAA-15, NOAA-16, NOAA-18, and AQUA.

The directory *\$SRC/Test-Data/ASCII tmp/gps AMSU Tbs/* contains the derived AMSU brightness temperatures from the COSMIC and CHAMP GPSRO missions. These are the input data used by the processing algorithm. The other directories; *extract/*, *match/*, *offset slope/*, and *bin/* in the *\$SRC/ASCII tmp/* directory contain the intermediate processing results from each IDL program for these two months. The final netCDF results are contained in the *\$SRC/Test-Data/Output/* directory.

## 4.2 Test Output Analysis

### 4.2.1 Reproducibility

Along with the two months of level 1B AMSU data and GPS RO derived brightness temperatures, all of the intermediate datasets generated during processing leading up to the final results are provided. Applying the processing algorithm to the input datasets, the user should recover exact results for each of these intermediate files. Differences in any of these intermediate or final results are indicative of an error.

### 4.2.2 Precision and Accuracy

#### a. Precision and Accuracy of RO Data

Kuo et al. (2004) showed that GPS RO soundings have very high accuracy (up to 0.3% in terms of refractivity) in the layer between 5 to 25 km. Ho et al., (2009a) showed that collocated CHAMP and COSMIC dry temperature differences between 500 hPa and 10 hPa range from -0.35 K (at 10 hPa) to 0.25 K (at 30 hPa) and their mean difference is about -0.034 K. The fact that the mean dry temperature difference in the height ranging from 500 hPa to 10 hPa is within the normalized standard error of the mean difference demonstrates long-term stability of the GPS RO signals. Since the AMSU forward model cannot introduce additional variability, the precision of these temperature measurements at altitudes sensitive to AMSU channel 9 results in stable reference values for channel 9 brightness temperatures.

To quantify the accuracy of RO temperature profile, we compared RO temperature profiles collocated with high quality radiosonde data. Temperature comparison between COSMIC and temperature measurements from Vaisala-RS92 show that COSMIC temperature is very close to those of radiosondes from 200 hPa to 20 hPa (around 12 km to 25 km) with a zero mean (He et al., 2009; Ho et al., 2010a).

## b. Precision and Accuracy of RO Derived AMSU TLS

We also quantify the accuracy of the defined slope and offset by finding the difference between COSMIC calibrated N18 AMSU Tbs ( $Tb_{\text{COSMIC\_N18}}$ ) and CHAMP calibrated N18 AMSU Tbs ( $Tb_{\text{CHAMP\_N18}}$ ); the  $Tb_{\text{CHAMP\_N18}}$  was found by comparing synthetic CHAMP Tbs ( $Tb_{\text{CHAMP}}$ ) to the collocated  $Tb_{\text{AMSU\_N18}}$  using the procedures introduced in Section 3. Again, CHAMP, COSMIC, N16 and N18 AMSU data from Sep. 2006 are used. The scatter plot for the CHAMP-N18 Tb comparison is shown in Fig. 5a and the slope and offset of the CHAMP-N18 pairs is defined. The  $Tb_{\text{CHAMP\_N18}}$  and  $Tb_{\text{COSMIC\_N18}}$  can be then computed using the following equations when N18 Tbs from CHAMP-N18 pairs are used as inputs:

$$Tb_{\text{CHAMP\_N18}} = 0.973 \times Tb_{\text{AMSU\_N18}} + 6.90 \quad (2)$$

$$Tb_{\text{COSMIC\_N18}} = 0.96 \times Tb_{\text{AMSU\_N18}} + 8.68. \quad (3)$$

The slope and offset defined in Eq. (3) are found using COSMIC-N18 pairs. Then we apply the same N18 Tbs from CHAMP-N18 pairs to Eqs. (2) and (3) to find  $Tb_{\text{COSMIC\_N18}}$  and  $Tb_{\text{CHAMP\_N18}}$ . Therefore, by finding the difference between  $Tb_{\text{COSMIC\_N18}}$  and  $Tb_{\text{CHAMP\_N18}}$ , we can determine if the slope and offset in Eq. (3) are still valid when different N18 Tbs are used as inputs. The scatter plot of  $Tb_{\text{COSMIC\_N18}}$  and  $Tb_{\text{CHAMP\_N18}}$  is shown in Fig. 5b. The correlation coefficient of  $Tb_{\text{CHAMP\_N18}}$  and  $Tb_{\text{COSMIC\_N18}}$  is equal to 1.0 and the mean bias between  $Tb_{\text{COSMIC\_N18}}$  and  $Tb_{\text{CHAMP\_N18}}$  is very close to zero ( $\sim 0.07$  K). The very tight fit of  $Tb_{\text{COSMIC\_N18}}$  and  $Tb_{\text{CHAMP\_N18}}$  (the standard deviation is about 0.1 K) demonstrates the consistency between the slope and offset (calibration coefficients) found in the N18-CHAMP pairs and that from N18-COSMIC pairs.

To see if we can find a similar conclusion for the GPS RO calibrated AMSU Tbs from other NOAA satellites, we repeat the above procedures but replace  $Tb_{\text{AMSU\_N18}}$  with  $Tb_{\text{AMSU\_N16}}$ , where COSMIC calibrated N16 AMSU Tbs ( $Tb_{\text{COSMIC\_N16}}$ ) and CHAMP calibrated N16 AMSU Tbs ( $Tb_{\text{CHAMP\_N16}}$ ) can be computed using the following equations when the same N16 Tbs from CHAMP-N16 pairs are used as inputs:

$$Tb_{\text{CHAMP\_N16}} = 0.984 \times Tb_{\text{AMSU\_N16}} + 4.05 \quad (4)$$

and

$$Tb_{\text{COSMIC\_N16}} = 0.978 \times Tb_{\text{AMSU\_N16}} + 5.50. \quad (5)$$

The scatter plots similar to Figs. 5a and 5b are shown in Figs. 5c and 5d, respectively. It is shown in Fig. 5c that we have fewer N16-CHAMP pairs when compared to that of N18-CHAMP pairs (Fig. 5a). This is because the distribution of CHAMP data is more synchronized to that of N18 than that of N16 in this month. The fact that the mean difference ( $-0.07$  K) and standard deviation ( $\sim 0.1$  K) between  $Tb_{\text{COSMIC\_N16}}$  and  $Tb_{\text{CHAMP\_N16}}$  is

compatible to those from  $Tb_{\text{COSMIC}_N18}$  and  $Tb_{\text{CHAMP}_N18}$  demonstrates that even with fewer samples (from CHAMP-N16 pairs in this month), because of the high precision of GPS RO data, we can still define robust slopes and offsets for NOAA-CHAMP pairs which are consistent with those derived from NOAA-COSMIC pairs.

Results in Figs. 5b and 5d can also be interpreted as an indirect estimate of the precision of the averaged  $Tb_{\text{COSMIC}}$  and  $Tb_{\text{CHAMP}}$  where N18/N16  $Tb$ s are used as cross references, although different N18/N16 samples are used for N18/N16-CHAMP and N18/N16-COSMIC pairs. This indicates that, even though we cannot directly compare  $Tb_{\text{COSMIC}}$  and  $Tb_{\text{CHAMP}}$ , by comparing  $Tb_{\text{COSMIC\_AMSU}}$  and  $Tb_{\text{CHAMP\_AMSU}}$ , where slopes and offsets from N18-COSMIC and N18-CHAMP pairs respectively are used, we can still define the precision between  $Tb_{\text{COSMIC}}$  and  $Tb_{\text{CHAMP}}$ . The  $\pm 0.07$  K mean differences of GPS RO-NOAA pairs and  $\sim 0.1$  K of standard deviation may still be related to the natural variability within 50 km separation distance and 30-minute time difference. In the future, more samples with a smaller time difference and separation distance will be used to provide better estimation of the mean difference and precision between  $Tb_{\text{COSMIC}}$  and  $Tb_{\text{CHAMP}}$ . A smaller mean bias and a higher precision between  $Tb_{\text{COSMIC}}$  and  $Tb_{\text{CHAMP}}$  can be expected.

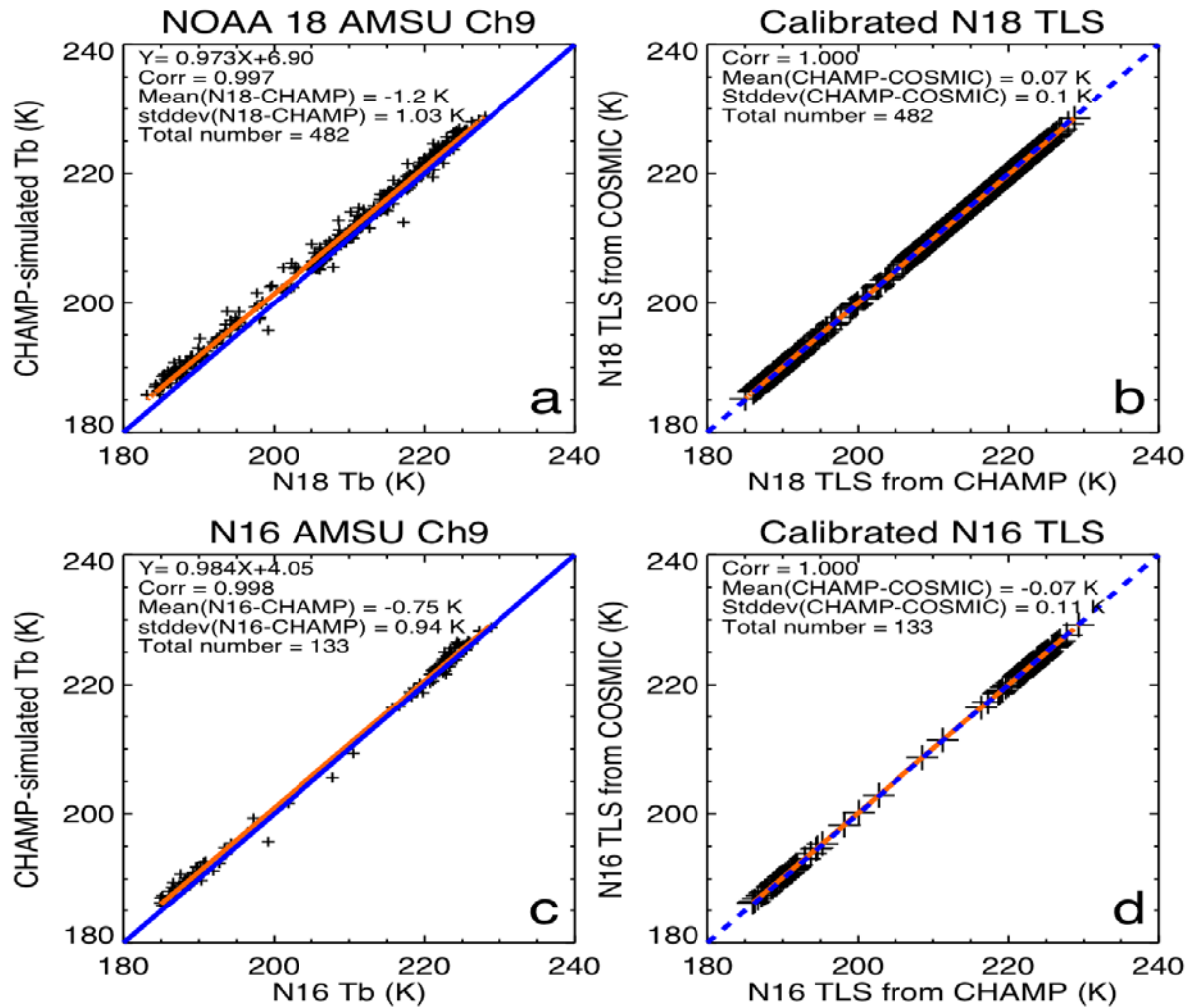


Figure 5: Comparison of (a) synthetic CHAMP Tbs and AMSU N18 Ch9 Tbs, (b) COSMIC calibrated N18 AMSU Tbs and CHAMP calibrated N18 AMSU Tbs, (c) synthetic CHAMP Tbs and AMSU N16 Ch9 Tbs, and (d) COSMIC calibrated N16 AMSU Tbs and CHAMP calibrated N16 AMSU Tbs.

### 4.2.3 Error Budget

N/A

## 5. Practical Considerations

### 5.1 Numerical Computation Considerations

IDL is not well suited to take full advantage of SMP environments. Since the computationally intense programs typically have to be run separately for each RO mission or polar orbiter, processing is optimized by simultaneously running separate IDL sessions.

### 5.2 Programming and Procedural Considerations

Execution of the IDL programs requires that the user edit the program file to specify the run parameters controlling execution. Programs must then be compiled and run from within an IDL session.

### 5.3 Quality Assessment and Diagnostics

To assess the quality of the derived TLS record, we compare the derived TLS record with other TLS datasets. Here we briefly introduce comparison results using the derived TLS record with the newly available TLS datasets provided by RSS (Remote Sensing System Inc.) and UAH (University of Alabama in Huntsville), and TLS processed by NOAA Center for Satellite Applications and Research (STAR, using simultaneous nadir overpass-SNO method) from 2001 to 2010. This is to demonstrate the quality of the derived TLS record.

#### a. Global Monthly Maps of RSS, UAH, STAR, and RO\_AMSU TLS

**Figure 6** shows the global monthly mean map in a 2.5 degree x 2.5 degree grid on January 2004 for RSS, UAH, SNO, and RO-simulated AMSU TLS.

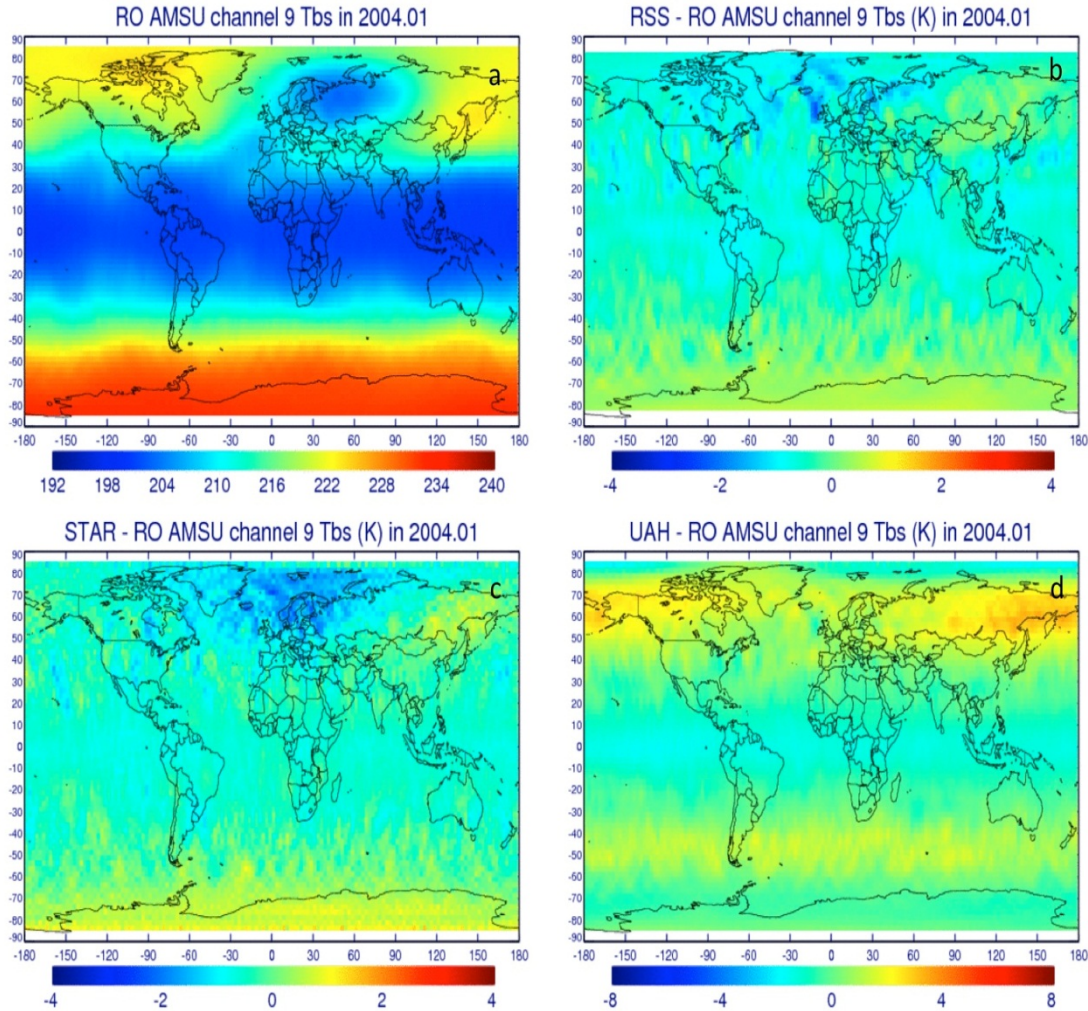


**Figure 6: The global monthly map in a 2.5 degree x 2.5 degree grid on January 2004 for (a) RO-simulated AMSU TLS, (b) RSS, (c) UAH, and (d) SNO.**

### **b. Time Series of RSS, UAH, STAR, and RO\_AMSU TLS Anomalies**

**Figure 7** shows that the time series of the TLS difference among RSS, UAH, and SNO relative to that of RO\_AMSU vary with different latitudinal zones. The TLS anomalies from SNO generally agree well with those from RO-calibrated AMSU TLS in all latitudinal zones.

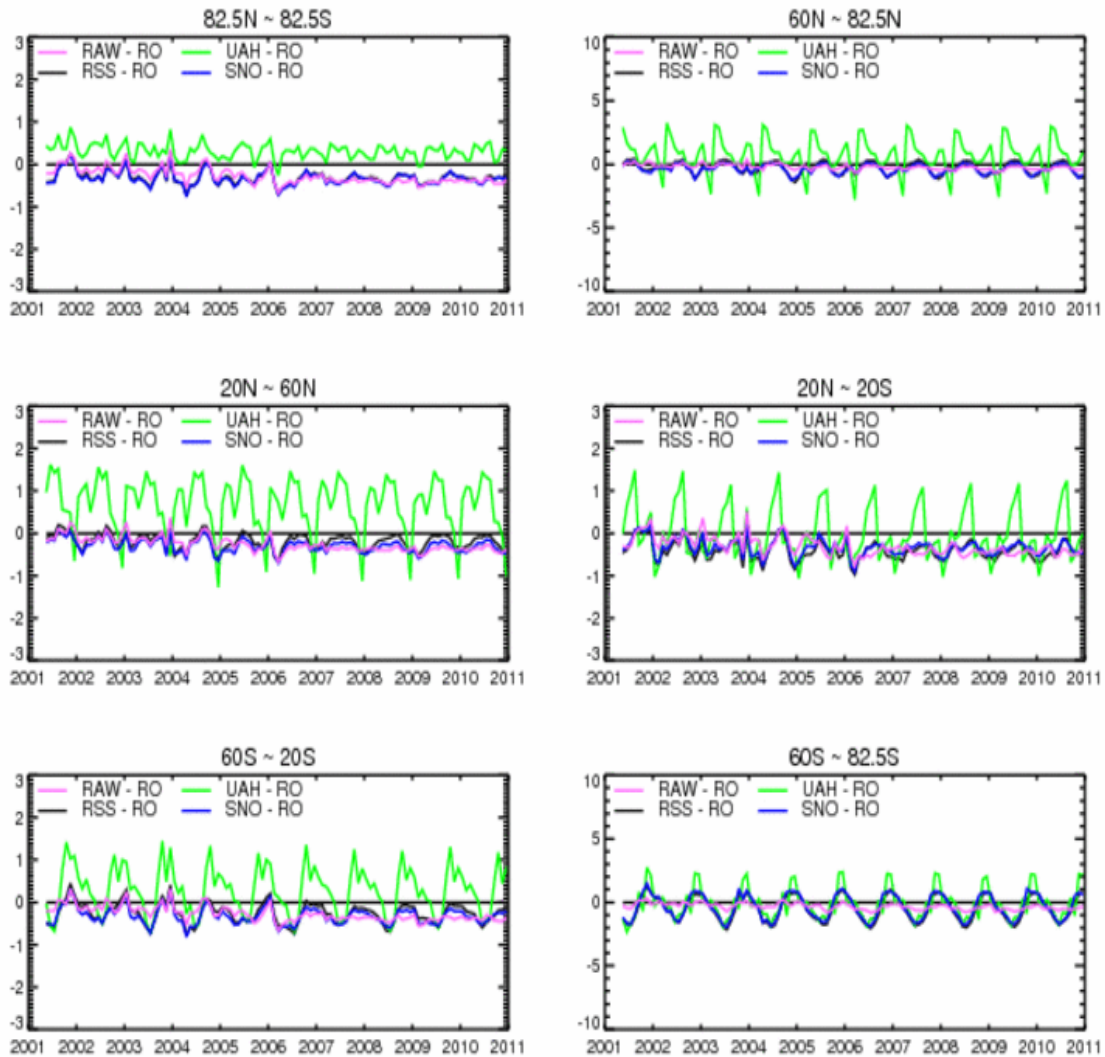


Figure 7: The time series of the TLS difference for RSS-RO\_AMSU, UAH-RO\_AMSU, and SNO-RO\_AMSU for (a) the entire globe (82.5°N-82.5°S, the left upper panel), (b) the 82.5°N-60°N zone (the upper right panel), (c) the 60°N-20°N zone (the middle left panel), (d) the 20°N-20°S zone (the middle right panel), (e) the 20°S-60°S zone (the bottom left panel), and (f) the 60°S-82.5°S zone (the bottom right panel).

## 5.4 Exception Handling

The program will stop and print out an informative message for all *known* error conditions.

## 5.5 Algorithm Validation

To further validate the calibration algorithm, we perform extra tests using RO and AMSU data as the following. Here we used a similar calibration method in this test study. RO simulated AMSU Tbs are used to further inter-calibrate the pixel level microwave Tbs (NESDIS<sub>OPR</sub>) from 2009 to 2012, and validate new available NEN<sub>NEW</sub> after 2006 according to the availability of the data. The calibrated MSU/AMSU TLS will be served as reference data to calibrate other overlapped MSU/AMSU data. Recently Ho et al., (2008b) has demonstrated the feasibility of this approach by examining whether the calibration coefficients (slope and offset) found from NOAA 15 (N15)- NOAA 16 (N16) pairs and N16-COSMIC pairs are consistent to that constructed from COSMIC-N15 pairs. This is to see if we have only N16-COSMIC pairs and N15-N16 pairs, how consistent is the constructed N15 Tbs (denoted as N16-calibrated N15 Tbs) and COSMIC-calibrated N15 Tbs. Figure 8 shows the comparison of COSMIC-calibrated N15 Tbs and N16-calibrated N15 Tbs. The very tight fit of the COSMIC-calibrated N15 Tbs and N16-calibrated N15 Tbs (with mean bias  $\sim 0.06\text{K}$  and standard deviation  $\sim 0.04\text{K}$ ) show that the calibration coefficients found from NOAA-NOAA pairs are also data are

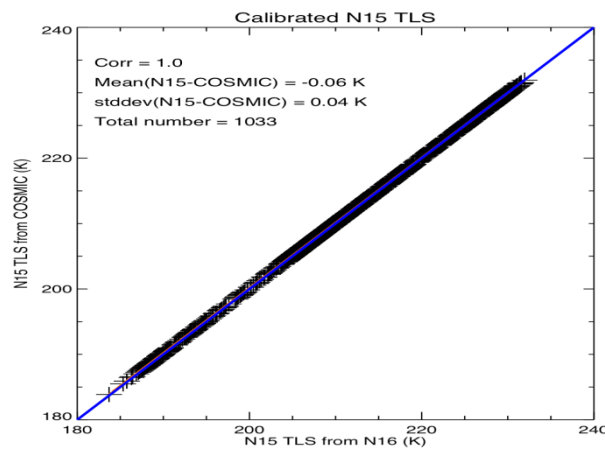


**Figure 8: Comparison of COSMIC-calibrated N15 Tbs and N16-calibrated N15 Tbs. The best fit is in dash line. Diagonal one-to-one fit is in gray solid line.**

consistent with that of NOAA-COSMIC pairs. This gives us confidence in using the RO-calibrated MSU/AMSU Tbs to calibrate other overlapped MSU/AMSU Tbs when RO not available.

The recommended approach to further validate the program will be to use RO data from multiple RO missions after 2012 to simulate AMSU Tbs and use the simulated AMSU Tbs to further inter-calibrate the pixel level microwave Tbs (NESDIS<sub>OPR</sub>) from multiple AMSU mission and inter-compare the consistency between the calibrated Tbs as above.

## **5.6 Processing Environment and Resources**

IDL version 7.1 was used to process the data on a x86\_64 server running the CentOS operating system. The ASCII temporary data files require about 7Gb of disk space per month.

## **6. Assumptions and Limitations**

The algorithm assumes that there are a sufficient number of coincident measurements during each month to provide a statistically reliable estimate of slope and offset values.

### **6.1 Algorithm Performance**

N/A

### **6.2 Sensor Performance**

N/A

## **7. Future Enhancements**

### **7.1 Enhancement 1**

For version 1.0 results, the AQUA orbiter was processed allowing only scan angles from -10 to +10 degrees. Though the impact on results is small, for version 1.1 the same scan angle range will be used for all orbiters.

### **7.2 Enhancement 2**

To avoid processing errors which result from the user having to edit and re-run programs for different GPSRO missions, polar orbiters, time intervals, etc., The algorithm should be restructured to utilize a single configuration file containing RUN parameters used by all of the processing programs. A single processing program should then implement the algorithm by calling each of the current processing programs as subroutines.

Programs should be restructured so that separate processing of AQUA is eliminated.

Intermediate data file should be stored in a more robust format which does not use so much disk space.

## 8. References

- Ackerman, S. *et al.* (1997). Discriminating clear-sky from cloud with MODIS: Algorithm Theoretical Basis Document, Version 3.2.
- Food and Agriculture Organization of the United Nations, Digital Soil Map of the World and Derived Soil Properties-Version 3.5, FAO/UNESCO, Rome, 1995.
- Friedl, M. A., and C.E. Brodley (1997). Decision tree classification of land cover from remotely sensed data. *Remote Sens. Environ.*, 61:399-409.
- Anthes, R. A., and Coauthors (2008), The COSMIC/FORMOSAT-3 Mission: Early Results. *Bul. Amer. Meteor. Soc.*, 89(3), 313-333.
- Bean, B.R., E. J., Dutton (1966), Radio Meteorology; National Bureau of Standards Monogr. 92; US Government Printing Office: Washington, DC, USA, 1966.
- Christy, J. R., R. W. Spencer, and W. D. Braswell (2000), MSU Tropospheric temperatures: Data set construction and radiosonde comparisons, *J. Atmos. Oceanic Tech.*, 17, 1153-1170.
- Christy, J. R., R. W. Spencer, W. B. Norris, W. D. Braswell, and D. E. Parker (2003), Error estimates of Version 5.0 of MSU/AMSU bulk atmospheric temperatures. *J. Atmos. Oceanic Technol.*, 20, 613-629.
- Christy, J. R., and W. B. Norris (2004), What may we conclude about global tropospheric temperature trends? *Geophys. Res. Lett.*, 31, L06211, doi:10.1029/2003GL019361.
- Foelsche, U., B. Pirscher, M. Borsche, G. Kirchengast, and J. Wickert (2009), Assessing the Climate Monitoring Utility of Radio Occultation Data: From CHAMP to FORMOSAT-3/COSMIC. *Terr. Atmos. Oceanic Sci.*, 20, 155-170.
- GCOS (2004), GCOS-92: Implementation Plan for the Global Observing System for Climate in Support of the UNFCCC. WMO/TD, No. 1219, 153pp.
- Grody, N. C., K. Y. Vinnikov, M. D. Goldberg, J. Sullivan, and J. D. Tarpley, Calibration of Multi-satellites observations for climate studies (2004), Microwave Sounding Unit (MSU), *J. Geophys. Res.*, 109, doi:10.1029/2004JD005079.
- Hajj, G. A., and Coauthors (2004), CHAMP and SAC-C atmospheric occultation results and intercomparisons. *J. Geophys. Res.*, 109, D06109, doi:10.1029/2003JD003909.
- He, W., S. Ho, H. Chen, X. Zhou, D. Hunt, and Y. Kuo (2009), Assessment of radiosonde temperature measurements in the upper troposphere and lower stratosphere using COSMIC radio occultation data, *Geophys. Res. Lett.*, 36, L17807, doi:10.1029/2009GL038712.
- Ho, S.-P., Y. H. Kuo, Zhen Zeng and Thomas Peterson (2007), A Comparison of Lower Stratosphere Temperature from Microwave Measurements with CHAMP GPS RO Data, *Geophys. Research Letters*, 34, L15701, doi:10.1029/2007GL030202.
- Ho, S.-P., M. Goldberg, Y.-H. Kuo, C.-Z Zou, W. Schreiner (2009a), Calibration of Temperature in the Lower Stratosphere from Microwave Measurements using COSMIC Radio Occultation Data: Preliminary Results, *Terr. Atmos. Oceanic Sci.*, Vol. 20, doi: 10.3319/TAO.2007.12.06.01(F3C).
- Ho, S.-P., G. Kirchengast, S. Leroy, J. Wickert, A. J. Mannucci, A. K. Steiner, D. Hunt, W. Schreiner, S. Sokolovskiy, C. O. Ao, M. Borsche, A. von Engeln, U. Foelsche, S. Heise, B. Iijima, Y.-H. Kuo, R. Kursinski, B. Pirscher, M. Ringer, C. Rocken, and T. Schmidt (2009b), Estimating the Uncertainty of using GPS Radio Occultation Data for Climate

- Monitoring: Inter-comparison of CHAMP Refractivity Climate Records 2002-2006 from Different Data Centers, *J. Geophys. Res.*, doi:10.1029/2009JD011969.
- Ho, S.-P., W. He, and Y.-H. Kuo (2009c), Construction of consistent temperature records in the lower stratosphere using Global Positioning System radio occultation data and microwave sounding measurements, in *New Horizons in Occultation Research*, edited by A. K. Steiner et al., pp. 207–217, Springer, Berlin, doi:10.1007/978-3-642-00321-9\_17.
- Ho, S.-P., Y. H. Kuo, W. Schreiner, X. Zhou (2010) Using SI-traceable Global Positioning System Radio Occultation Measurements for Climate Monitoring [In “States of the Climate in 2009”]. *Bull. Amer. Meteor. Sci.*, in press.
- Kuo, Y. H., T. K. Wee, S. Sokolovskiy, C. Rocken, W. Schreiner, D. Hunt, 2004: Inversion and Error Estimation of GPS Radio Occultation Data. *J. of the Meteor. Society of Japan*, 82(1B), 507-531.
- Mears, C. A., M. C. Schabel, and F. J. Wentz (2003), A reanalysis of the MSU channel 2 tropospheric temperature record, *J. Climate*, 16, 3650–3664.
- Mo. T., M. D. Goldberg, D. S. Crosby, and Z. Cheng (2001), Recalibration of the NOAA Microwave Sounding Unit, *J. Geophys. Res.*, **106**, 10145-10150.
- National Research Council, Committee on Earth Science and Applications from Space: A Community Assessment and Strategy for the Future (2007), *Earth Science and Application from Space: National Imperatives for the Next Decade and Beyond*, National Academies Press, 2007, 456 pp.
- Ohring, G., Ed., (2007), *Achieving Satellite Instrument Calibration for Climate Change*. National Oceanographic and Atmospheric Administration, 144 pp.
- Vinnikov, K. Y., and N. C. Grody (2003), Global Warming Trend of Mean Tropospheric Temperature Observed by Satellites, *Science*, **302**, 269-272.
- Vinnikov, K. Y., N. Grody, A. Robock, R. J. Stouffer, P. D. Jones, and M. D. Goldberg (2006), Temperature Trends at The Surface and in The Troposphere, *J. Geophys. Res.* **111**, D03106, doi:10.1029/2005JD006392, 1-14.
- Ware, R., and Coauthors (1996), GPS sounding of the atmosphere from low Earth orbit: Preliminary results. *Bull. Amer. Meteor. Soc.*, 77, 19–40.
- WMO, 2007: Final Report for Workshop on the Redesign and Optimization of the Space-based Global Observing System. WMO Headquarters, Geneva.
- Woolf, H., P. van Delst, W. Zhang (1999), NOAA-15 HIRS/3 and AMSU Transmittance Model Validation. Technical Proceedings of the International ATOVS Study Conference, 10th, Boulder, CO, 27 January-2 February 1999. Bureau of Meteorology Research Centre, Melbourne, Australia, 1999, pp.564-573.
- Zou, C. Z., M. Goldberg, Z. Cheng, N. Gordy, J. Sullivan, C. Cao, and D. Tarpley (2006), Recalibration of microwave sounding unit for climate studies using simultaneous nadir overpass. *J. Geophys. Res.* 111, D19114, doi:10.1029/2005JD006798.

## Acronyms and Abbreviations

| Acronym or Abbreviation | Meaning  |
|-------------------------|--|
| AMSU                    | Advanced Microwave Sounder Unit  |
| Auqa                    | Aqua (EOS PM-1) is a multi-national <u>NASA</u> scientific research <u>satellite</u> in <u>orbit</u> around the <u>Earth</u> |
| CATBD                   | Climate Algorithm Theoretical Basis Document   |
| CDR                     | Climate Data Record  |
| CHAMP                   | Challenging Mini-satellite Payload   |
| CIMSS                   | Cooperative Institute for Meteorological Satellite Studies   |
| COSMIC                  | Constellation Observing System for Meteorology, Ionosphere, and Climate  |
| GCOS                    | Global Climate Observing System  |
| GPS                     | Global Positioning System  |
| GRACE                   | Gravity Recovery And Climate Experiment  |
| IDL                     | Interface description language. This is a <u>specification language</u> used to describe a software component's interface    |
| LECT                    | Local equator crossing times   |
| LEO                     | low-Earth orbiting   |
| MetOP-A                 | METeorological Operational satellite-A   |
| MSU                     | Microwave Sounding Unit  |
| MWF                     | Microwave Forward Model  |
| NASA                    | National Aeronautics and Space Administration  |
| NCDC                    | National Climatic Data Center  |
| NESDIS                  | National Environmental Satellite, Data, and Information Service  |
| NOAA                    | National Oceanic and Atmospheric Administration  |
| NRC                     | National Science Council   |
| RO                      | Radio Occultation  |
| RSS                     | Remote Sensing System Inc.   |
| SI                      | System of Units  |
| SNO                     | Simultaneous Nadir Overpass  |
| SSEC                    | Space Science Engineer Center  |

| <b>Acronym or Abbreviation</b> | <b>Meaning</b>                                 |
|--------------------------------|--|
| STAR                           | Center for Satellite Applications and Research |
| Tb                             | Brightness Temperatures                        |
| TLS                            | Temperatures in the Lower Stratosphere         |
| UAH                            | University of Alabama in Huntsville            |